



Research article

Synthesis characterization and application of butyl acrylate mediated eco-friendly silver nanoparticles using ultrasonic radiation

Indu Saxena^{*}, Syed Mohammad Ejaz, Aditya Gupta*Department of Chemistry, University of Lucknow, Lucknow, 226007, India*

ARTICLE INFO

Keywords:

Silver nanoparticles
Ultra-sonication
Powder X-ray diffraction
Transmission electron microscopy
Dye degradation

ABSTRACT

In the present investigation, with an effort to provide appropriate material for future applications, we have touched on two viable advancement targets: the production of silver nanoparticles (Ag-NPs) employing an ultrasonic approach and the use of Ag-NPs in environmental remediation. A green economical method was involved to prepare Ag-NPs using butyl acrylate as a stabilizer. The following techniques were used for analysing Ag-NPs: energy dispersive X-ray spectroscopy (EDX), transmission electron microscopy (TEM), field emission scanning electron microscopy (FESEM), powder X-ray diffraction (XRD), and Fourier transformed infrared (FT-IR) spectroscopy. X-ray diffraction (XRD) analysis for the lattice characteristics showed that Ag-NPs have a face-centered structure with an average crystallite size of 9.51–11.83 nm. FE-SEM and TEM analysis were used for morphological investigations, and revealed that Ag-NPs had a spherical shape with an average particle size of 16.27 nm. The EDX profile displayed a strong signal at ~3.0 keV, which indicated that the samples comprised silver. UV-Visible spectrophotometer with the absorption maximum occurring between 401 and 411 nm further confirmed the formation of Ag-NPs. The dye degradation effect of synthesized Ag-NPs on methylene blue and Rhodamine B was analyzed to assess their ability for environmental remediation, and results showed that around 100% of the dye degradation effect. This study has provided a most plausible mechanism for the dye degradation.

1. Introduction

Over the last decades, refined attention has been devoted to nanomaterials synthesis and applications. Nanoparticles (NPs) of noble metals like silver, gold, palladium etc., played crucial role in different biological, chemical and physical assets from their bulk counterparts due to their unique physicochemical properties [1–5]. In recent times researchers have a great interest in nano-size materials (less than 100 nm) as they exhibited huge utility in several areas of industry, for instance, toothpaste, coating of refrigerators, food storage, cellular phones, air sanitizer spray, washing machines, detergents, soaps, etc. [6–9]. In general, the intrinsic assets of metal NPs are mainly ascertained through their composition, crystallinity, size, and structure [6,10]. Discoveries in the last few years have noticeably confirmed that the optical, electromagnetic, and catalytic properties of silver nanoparticles (Ag-NPs) are intensely affected by size and shape distribution, which are frequently diverse by differing the synthetic methods, reducing agents and

^{*} Corresponding author.

E-mail addresses: indu.anv@gmail.com, indu_lu@yahoo.com (I. Saxena).

stabilizers [11–16]. From literature survey, it has been clear that Ag-NPs displayed a broad spectrum of biological activities such as antibacterial, antifungal, and anti-cancer etc., [17]. A lot of methods have been described for the synthesis of nanomaterials for example Ag-NPs are usually synthesized by chemical reduction method. However, irradiation of ultrasonic, microwave, gamma, and UV rays have also been one of the ways for synthesizing Ag-NPs [18,19]. The ultrasonic method has been one of the most popular methods for a synthesizing variety of noble metal NPs including Ag, Au, Pt, Pd, etc., as well as other nanomaterials [20]. A lot of studies reported the formation of Ag-NPs via ultrasonic method as it was found to be much simple, eco-friendly, cost-effective, and a favorable pathway for the synthesis of fine metal nanoparticles with desired size and structure [21–24]. In this study, we synthesise Ag-NPs because there are numerous advantages to adopting the ultrasonic approach. Ag-NPs in aqueous or ethanoic media are previously synthesized for the majority of researchers. Consequently, an effort has been undertaken utilising polymeric media, i.e., the synthesis of Ag-NPs in butyl acrylate medium. Butyl acrylate is an inexpensive natural monomer and can behave as a good stabilizer for Ag-NPs. Water remediation is a major global concern these days due to the significant health and environmental risks it poses to human life. Organic dyes or dye-based effluent which are toxic with non-biodegradable properties caused water pollution which is an imminent worldwide problem [25]. Because dyes are used in many fields, such as the textile, food, and leather industries, several processes, such as coagulation, flocculation, chemical precipitation, biodegradation, ozonation, solvent extraction, ion exchange, membrane filtration, electrochemical destruction, and adsorption, have been developed to reduce dye pollutants and protect the environment and aquatic life [25,26]. Unfortunately, these methods have high operating costs and are ineffective in accomplishing the complete elimination of organic dyes from wastewater [25,27–30].

In the present study, we reported a greener technique for Ag-NPs synthesis by changing the concentrations of butyl acrylate under ultrasonic irradiation at room temperature for 2 h. The as-synthesized Ag-NPs are characterized using UV–Visible spectroscopy, powder X-ray diffraction (XRD), transmission electron microscopy (TEM), field emission scanning electron microscopy (FESEM), energy dispersive X-ray spectroscopy (EDX), and Fourier transformed infrared (FT-IR) spectroscopy. The as-synthesized Ag-NPs are subjected to test its catalytic action for dye degradation.

2. Experimental protocol

2.1. Materials

Silver nitrate (99.89%) was purchased from Bendosen (C0721-2284551), India. In addition, Butyl acrylate, grad type (CAS 9000-07-1), was purchased from Sigma-Aldrich (St. Louis, MO, USA). Methylene blue (MB), Rhodamine B (RhB), and NaBH_4 were purchased from Sigma-Aldrich. All chemicals were used without further treatment in the entire synthesis process. All stock solutions were prepared by using double distilled water and aqua regia was used to wash glassware properly, then autoclaved and sanitized.

2.2. Synthesis of silver nanoparticles

A variety of Ag-NPs were synthesized by mixing 10 ml AgNO_3 (0.1 M) in 40 ml of 0.10, 0.15, 0.20, 0.25, and 0.3 wt % butyl acrylate solutions on a magnetic stirrer for 2 h at room temperature. The samples were then exposed to high-intensity ultrasonic irradiation at room temperature for 2 h at 50 % amplitude. It has been found that the solution turned to yellowish brown from colorless which confirms the formation of Ag-NPs. The suspensions were then centrifuged for 15 min and rinsed three-four times with double distilled water to eliminate the silver ion residue as well as impurities. The powdered Ag-NPs were collected from the decantation of water and then dried at 100 °C under a vacuum overnight.

2.3. Catalytic degradation of dyes

Freshly prepared (0.1 M) sodium borohydride and stock solution of rhodamine B or methylene blue (10 mg/L) were used. To test the catalytic degradation of dye, 0.5 ml of the stock solution of borohydride and 0.5 ml of Ag-NP are separately injected into Rhodamine B or methylene blue solution. Theb the samples were incubated for a day and subjected to record absorption spectra using UV–Vis spectrophotometer.

2.4. Instrumentation

The absorption spectra of Ag-NPs were recorded on a Lab UV next-generation UV–visible double beam spectrophotometer over a wavelength range of 300–900 nm. For structural analysis, the X-ray diffractometer (Rigaku smart lab X-ray diffractometer with Cu K_α radiation ($\lambda = 1.5404 \text{ \AA}$) in the 2θ range from 10° to 85° with a step of 0.5° per minute was used. A series 100 PerkinElmer FT-IR 1650 spectrophotometer was used to record FT-IR spectra in the range of 500–4000 cm^{-1} (PerkinElmer, Waltham, MA, USA). The entire structure and size of synthesized Ag-NPs were examined with the help of FE-SEM with a JEOL JSM 761 working at 0.5–30 kV and HR-TEM with an FEI Tecnai running at 0.5–30 kV.

3. Results and discussion

The suspension of butyl acrylate and AgNO_3 solution was light yellow; when exposed to ultrasonic irradiation at 50 % amplitude for

2 h at room temperature, the color changed from light yellow to yellowish-brown solution, showing Ag-NPs formation [31]. The most plausible mechanism for Ag-NPs synthesized by butyl acrylate has been shown in Scheme 1, equations 1- 6. On application of ultrasonic waves, water splits and leads to the formation of hydrogen and hydroxide free radicals (eq 1) [20,32,33]. These radicals are capable of giving sufficient chemical potential to produce nanoparticles via the reduction of noble metals. The hydroxide free radical in turn combines with butyl acrylate (RH) and leads to the formation of R free radical (eq 2) [34]. However, equation 3 demonstrated the hydrolysis of silver nitrate aqueous solution which leads to produce Ag^+ and NO_3^- ions [19]. The R free radical produced in the reaction mixture simultaneously reacts with Ag^+ ions and hence reduction of Ag^+ into Ag^0 takes place (eq 4) with the formation of R' [35]. Similarly, the remaining amount of silver ions reacts with the hydrogen-free radical (produced in eq 1) to reduce it into Ag^0 or Ag-NPs (eq 5) [36]. Further, few remaining Ag^+ interact with the as-formed Ag^0 and leads to produce quite aggregated Ag-NPs [37].

3.1. XRD study of synthesized silver nanoparticles

The structural properties and crystallite size of the Ag-NPs were analyzed by powdered X-ray diffraction (XRD) technique. The XRD pattern for various concentrations i.e. 0.10, 0.15, 0.20, 0.25, and 0.30 % of butyl acrylate polymer used for the formation of Ag-NPs was shown in Fig. 1(i). The XRD pattern of Ag-NPs reveals several characteristics peaks in the broad-angle range of 2θ from 20° to 85° with step size 0.5° per minute with Cu-K_α radiation. It revealed almost same XRD pattern for each variation of butyl acrylate polymer with a prominent change in the intensity of Bragg's peaks. The XRD peaks at 2θ values 38.22° , 44.39° , 64.69° , 77.62° , and 82.22° can be allocated to the (111), (200), (220), (311), and (222) crystallographic plane of silver crystals, respectively, which is in agreement with the JCPDS file number 04-0783 of silver [36,38]. It revealed a face-centered cubic structure of the synthesized Ag-NPs with the most of the crystallites oriented towards (111) plane. The Ag-NPs are extremely crystalline which implies that this method produced high-purity Ag-NPs [39,40]. The average crystallite size "D" of the synthesized Ag-NPs was evaluated by Scherer's formula given by equation (7) [41,42];

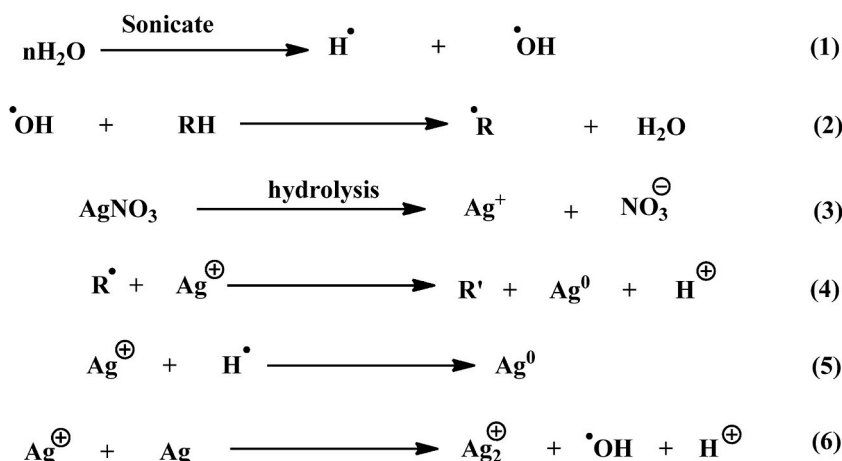
$$D = \frac{0.9\lambda}{\beta \cos \theta} \quad (7)$$

Where β is FWHM (full width at half maxima), shape factor is 0.9, wavelength λ is (1.5404 Å, Cu-K_α), and θ is the diffraction angle.

Since most of the crystalline were oriented towards the (111) plane, therefore, the average crystallite size was calculated concerning (111) plane of each diffraction pattern. Table 1 represents the calculated D for each variation of butyl acrylate in the reaction mixture. The D-value varied from 9.51 to 11.83 nm depending upon the concentration of butyl acrylate in the reaction mixture. Additionally, a plot in Fig. 1(ii) has been plotted to study the change in average crystallite with the variation of butyl acrylate polymer concentration and it suggested that the average crystallite size decreases as the concentration of butyl acrylate solution increases. But the change in the average crystallite size of Ag-NPs was not considerable. So, any concentration of butyl acrylate polymer of the present study can be used for Ag-NPs formation of 9.51–11.83 nm sized which may be further used for multipurpose applications.

3.2. EDX analysis

EDX profile of the synthesized Ag-NPs was recorded by energy-dispersive X-ray spectroscopy. Fig. 2(a–e) illustrated the EDX profile of Ag-NPs prepared by using 0.10, 0.15, 0.20, 0.25, and 0.3 % butyl acrylate concentrations, respectively. It shows signals corresponding to silver and oxygen at ~ 3.0 and < 1.0 KeV, respectively [42], which confirms the presence of silver in the analyzed samples and showed a good resemblance with the result of XRD analysis. The presence of oxygen in analyzed Ag-NPs might be due to the adsorption of R' group onto its surface or aerial oxidation of some silver ions [42]. No other impurity-related signal was found in the



Scheme 1. Proposed mechanism for Ag-NPs formation.

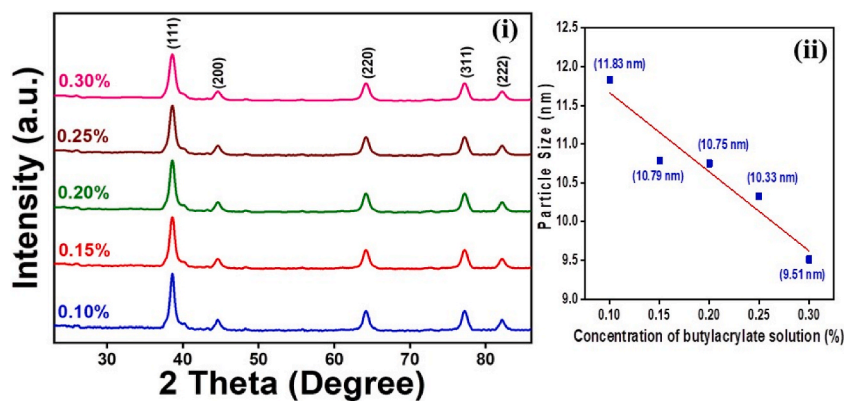


Fig. 1. (i) XRD plot for the Ag-NPs at different concentration of butyl acrylate (0.1, 0.15, 0.2, 0.25, and 0.3 %) (ii) Average crystallite size vs concentration of butyl acrylate solution (%).

Table 1
Average crystallite size (D) calculated via XRD plot.

Concentration of Butyl acrylate solution (in %)	Average Crystallite size (D) (in nm)
0.10	11.83
0.15	10.79
0.20	10.75
0.25	10.33
0.30	9.51

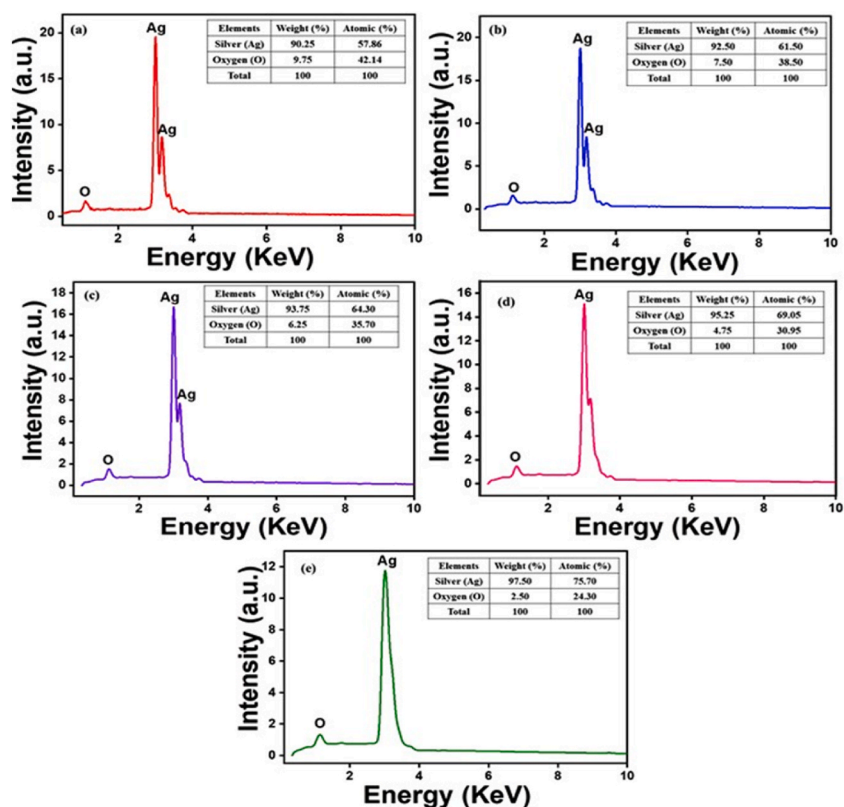


Fig. 2. (a–e) EDX profile for Ag-NPs at different concentration of butyl acrylate (a) 0.1% (b) 0.15% (c) 0.2% (d) 0.25% (e) 0.3%.

EDX, demonstrating that the NPs are entirely comprised of silver and oxygen. The elemental composition of silver and oxygen in each sample was shown in Table 2. It revealed that with an increase in butyl acrylate concentration in the reaction mixture, the percentage weight composition of silver increases. Conclusively, 0.30 % concentration of butyl acrylate was optimized for the formation of Ag-NPs via the ultrasonic method.

3.3. Field emission scanning electron microscopy (FE-SEM)

To analyse the morphology and particle size (average) of the synthesized Ag-NPs, FE-SEM analysis was carried out and the images captured for different concentrations of butyl acrylate i.e. 0.10, 0.20, 0.25, and 0.30 % are shown in Fig. 3(a–e), respectively. These images revealed that the spherical-shaped Ag-NPs were formed. Also, as the concentration of butyl acrylate in the reaction mixture increases, the small particle size Ag-NPs was observed in Fig. 3(a–e), which shows good resemblance with EDX data. Noticeably, agglomeration of Ag-NPs enhanced with the decrease in the particle size or at higher concentration of butyl acrylate. Furthermore, ImageJ software has been used to determine the average particle size (data listed in Table 3) of synthesized Ag-NPs. A graph has been plotted for comparing the average particle size of Ag-NPs for the concentration of butyl acrylate and it has been found that Ag-NPs are formed in the range of 27–60 nm size. This size range is good enough to use synthesized Ag-NPs in catalytic applications. However, to confirm exact particle size and morphology transmission electron microscopy analysis was performed.

3.4. Transmission electron microscopy (TEM)

The images captured using TEM are shown in Fig. 4(i)–(a–e) at 50 nm scale. From TEM images it has been clear that Ag-NPs have a spherical morphology and are quite agglomerated in the medium. To evaluate the average particle size ImageJ software has been used and particle size distribution plots have been drawn, Fig. 4(ii)–(a–e). Based on particle size distribution plots, summarized values of the average particle size of each sample are listed in Table 4. The average particle size was found in the range of 16–28 nm. It also revealed that as the concentration of butyl acrylate in the reaction mixture increases, the particle size of the synthesized Ag-NPs decreases which showed good resemblance with the results of XRD, SEM, and EDX. Also, the agglomeration of NPs considerably decreases as the concentration of butyl acrylate is enhanced. Conclusively, the synthesized Ag-NPs with particle size of below 30 nm are promising material for multipurpose applications [42]. Therefore, the synthesized Ag-NPs are employed to test their catalytic activity in methylene blue and rhodamine dye degradation reactions.

3.5. Optical properties analysis

The absorption spectra of Ag-NPs at different concentrations of butyl acrylate are displayed in Fig. 5(i) (a–e). The absorption spectra are helpful in confirmation of the Ag-NPs formation and are shown in Fig. 5 (i, ii, iii). The absorption spectrum displayed strong absorptions in the wavelength range of 401–411 nm which matched well with the surface plasmonic band of Ag-NPs [37,43]. From Fig. 5(i), it is clear that the intensity of the absorption peak increases with increasing butyl acrylate concentrations (0.1, 0.15, 0.2, 0.25, and 0.30% [44]. Furthermore, Fig. 5(ii) revealed that when butyl acrylate concentration increased, the absorbance also increased, and the absorption maxima were shifted towards a lower wavelength i.e., a blue shift occurs which infers that the particle size of synthesized Ag-NPs reduced considerably [45,46]. Similarly Fig. 5 (iii) showed the change in absorbance of the sample as the concentration of butyl acrylate increases and it has been found that increases absorbance has been noticed for 0.30% butyl acrylate containing reaction mixture, refers larger particle size, which again matched well with the result of other technique. According to Mie's theory [47], different sizes of nanoparticles should have various optical properties due to differences in absorbance bands.

3.6. FT-IR analysis

The functional groups adsorbed on the surface of Ag-NPs were examined by FT-IR spectrum. Fig. 6 represented FT-IR spectra (a–e) of Ag-NPs with different butyl acrylate concentrations 0.10, 0.15, 0.20, 0.25, and 0.30 %, respectively. The characteristic sharp spectrum exhibited, the absorption at 3568–3579 cm^{-1} for O–H stretching vibration, 1425–1439 cm^{-1} for O–H bending vibration of carboxylic group, bands absorbed at 1058–1075 cm^{-1} absorption of strong tri substituted C–H bending vibration bands at 879–897 cm^{-1} and a strong monosubstituted C–H bending vibration bands absorbed at 746–759 cm^{-1} [48,49]. The sharp peak of Ag-NPs at 423 to 410 cm^{-1} was assigned for successful preparation of Ag-NPs. Furthermore, the shift in wavenumber of Ag-NPs samples to lower wave numbers with the increase in butyl acrylate concentration denoted that butyl acrylate and Ag-NPs are interacting strongly

Table 2
Elemental composition of Ag-NPs at different concentration of butyl acrylate.

Elements	0.10%		0.15%		0.20%		0.25%		0.30%	
	Weight (%)	Atomic (%)								
Silver (Ag)	90.25	57.86	92.50	61.50	93.75	64.30	95.25	69.05	97.50	75.70
Oxygen (O)	9.75	42.14	7.50	38.50	6.25	35.70	4.75	30.95	2.50	24.30

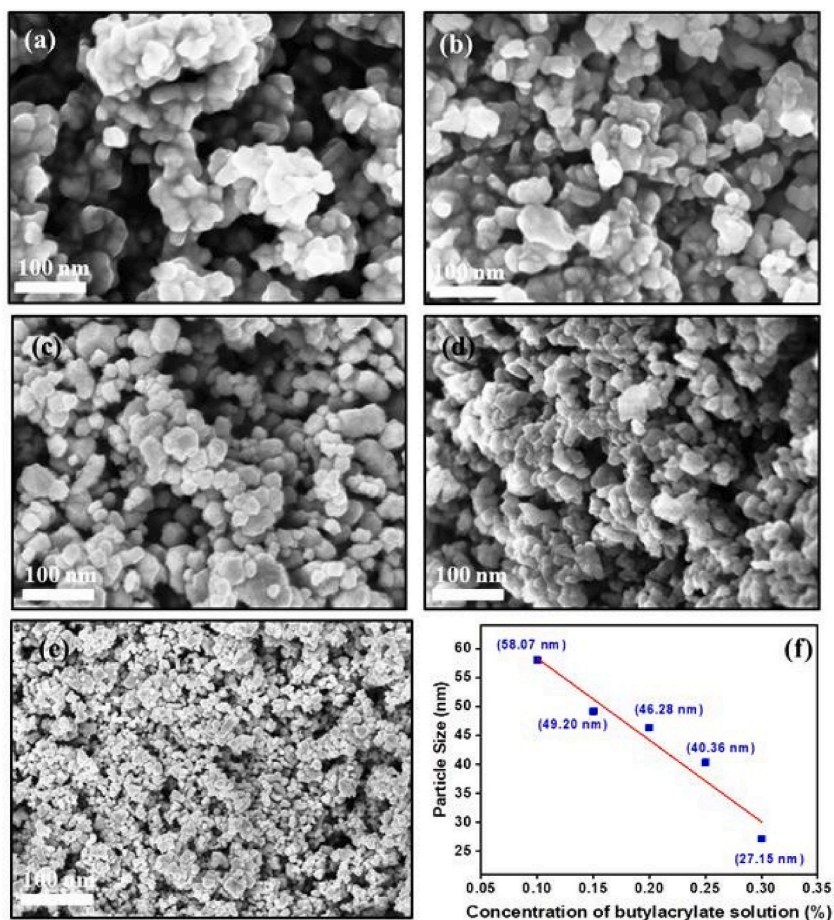


Fig. 3. (a–e) FE-SEM images for the Ag/butyl acrylate at different concentration of butyl acrylate [0.1% 4(a), 0.15% 4(b), 0.2% 4(c), 0.25% 4(d), and 0.3% 4(e)] and (f) mean particle size vs concentration of butyl acrylate solution (%).

Table 3

Average particle size of Ag-NPs calculated using FE-SEM images.

Concentration of butyl acrylate solution (%)	Average Crystalline size (D_{FE-SEM} (nm))
0.10%	58.07
0.15%	49.20
0.20%	46.28
0.25%	40.36
0.30%	27.15

[50–52].

3.7. Catalytic degradation of rhodamine B and methylene blue

The exploration of catalytic activity of the synthesized Ag-NPs was performed on the degradation of two toxic dyes namely Rhodamine B and methylene blue [50,51]. The absorbance spectra recorded for methylene blue dye degradation was shown in Fig. 7. The absorption peak corresponding to 665 nm, was used to determine the concentration change during the degradation process. The degradation of MB using NaBH_4 without any catalyst showed a very slow progress (more than a day), but when Ag-NPs added into the reaction takes place rapidly (within 18 h). The absorption spectra of MB show a sharp peak at 665 nm (Fig. 7) and upon reaction with Ag-NPs, the absorbance at this particular wavelength continuously decreases due to the degradation of dye along with the formation of degradation products such as CO_2 , H_2O [52,53]. To calculate the percentage of dye degradation the following formula (8) has been used

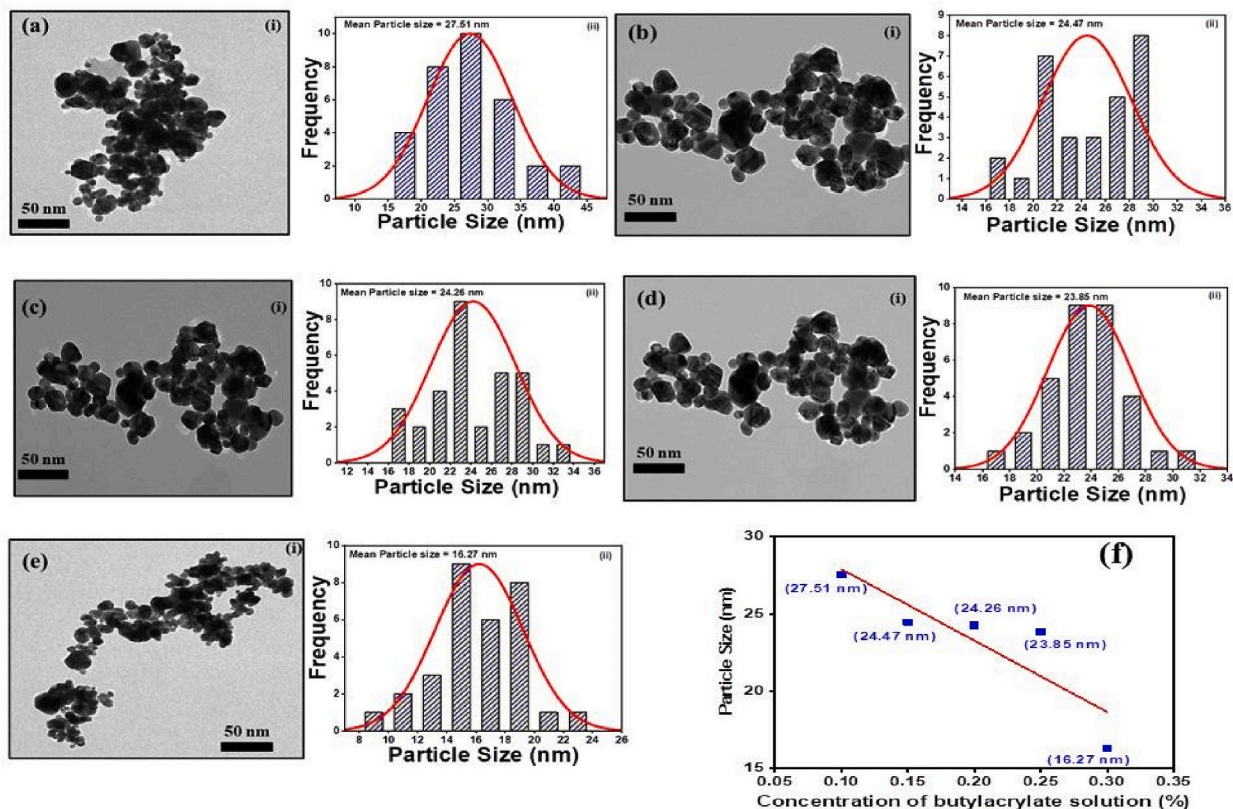


Fig. 4. (a–e) The particle size distribution for the Ag/butyl acrylate and TEM images at various concentrations of butyl acrylate [0.1% 4(a), 0.15% 4(b), 0.2% 4(c), 0.25% 4(d), and 0.3% 4(e)] and 4(f) mean particle size vs concentration of butyl acrylate solution (%).

Table 4
Average particle size of Ag-NPs calculated using TEM images.

Concentration of butyl acrylate solution (%)	Average particle size (in nm)
0.10	27.51
0.15	24.47
0.20	24.26
0.25	23.85
0.30	16.27

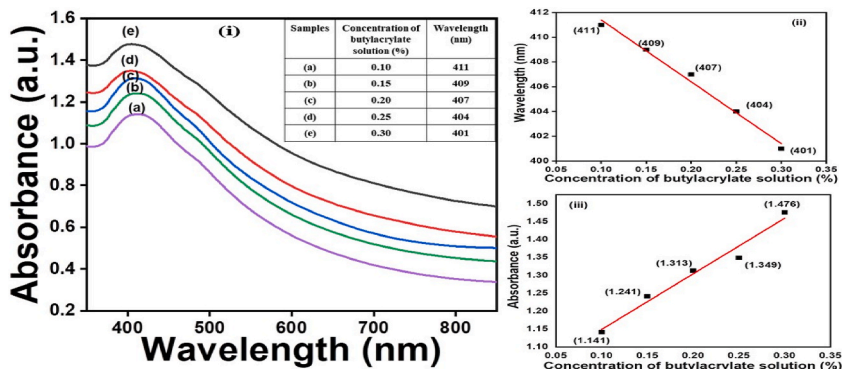


Fig. 5. (i) UV–Vis spectra for the Ag/butyl acrylate at different concentrations of butyl acrylate [0.1% (a), 0.15% (b), 0.2% (c), 0.25% (d), and 0.3% (e)] and (ii & iii) Wavelength & absorbance vs concentration of butyl acrylate solution (%).

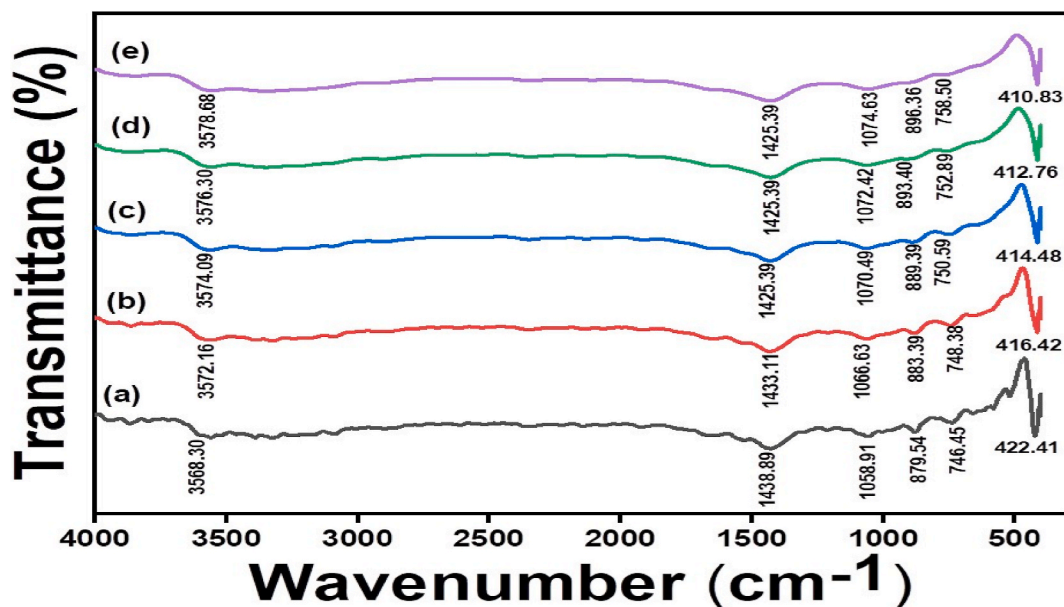


Fig. 6. FTIR spectra for the Ag-NPs at different concentrations of butyl acrylate [0.1% (a), 0.15% (b), 0.2% (c), 0.25% (d), and 0.3% (e)].

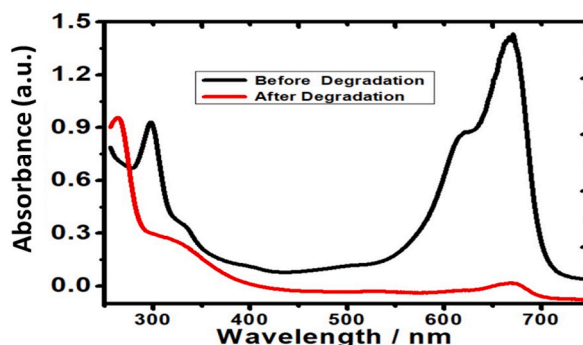


Fig. 7. Absorption spectra for methylene blue degradation. (For interpretation of the references to color in this figure legend, the reader is referred to the Web version of this article.)

$$\% \text{ dye degradation} = \left(\frac{A_{com} - A_{deg}}{A_{com}} \right) \times 100 \quad (8)$$

The color of the dye delocalizes which also confirms degradation. The % dye degradation of methylene blue was calculated as 100 % which confirms the synthesized Ag-NPs can be a good catalyst for MB dye degradation.

Likewise, Fig. 8 represented the absorption spectra recorded for the catalytic action of Ag-NPs on Rhodamine B dye, which possesses a peak at 665 nm. The intensity of this peak will decrease along with the decolorization of the solution confirming the degradation of Rhodamine B. The degradation of Rhodamine B is confirmed by the disappearance of the absorption peak at 665 nm.

The % dye degradation was calculated by using equation (8) and it has been found that 100 % degradation of rhodamine B occurred, which suggested that the synthesized Ag-NPs are good for the degradation of rhodamine B dye. The mechanism for the action of Ag-NPs upon dye degradation is shown in Fig. 9. Ag-NPs played a significant role in the catalytic reduction of dyes because it has a larger surface area and easily provides electron [45–47].

Due to the absorption of free electron of Ag-NPs, electron get excited and combined with O_2 and leads to form O_2^- which in turn reacts with H_2O and produces H_2O_2 . This H_2O_2 breaks its OH free radical and leads to reduce the dye along with the formation of the degradation products such as CO_2 , H_2O , etc. [54].

4. Conclusion

In summary, this research report demonstrated the synthesis of silver nanoparticles using butyl acrylate polymer as a stabilizing

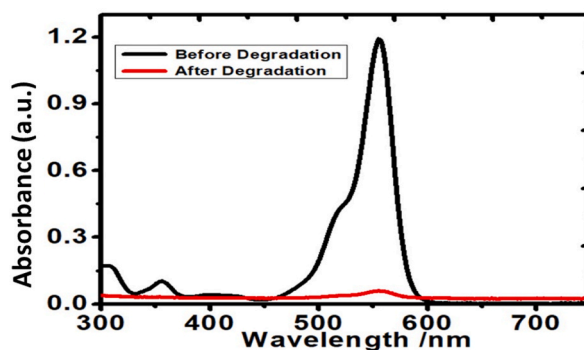


Fig. 8. Absorption spectra for Rhodamine B degradation.

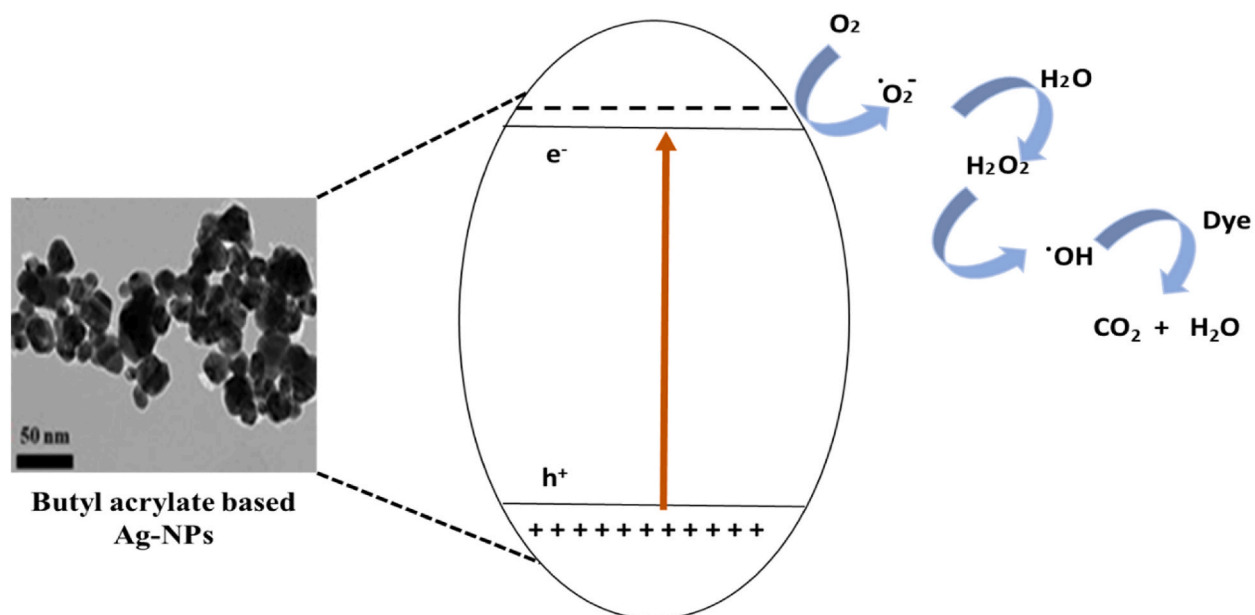


Fig. 9. Mechanistic action of Ag-NPs upon dye degradation.

agent via ultrasonic method. It involves a low-cost and nontoxic method for synthesis. The XRD examination revealed that Ag-NPs have a face-centered structure with an average crystalline size in the range of 9.51 and 11.83 nm. EDX profile confirmed the formation of Ag-NPs with no impurities in the synthesized samples. The surface area of Ag-NPs changed with increasing butyl acrylate concentration, resulting in small-sized Ag-NPs with a spherical shape (FE-SEM). The TEM images demonstrate that the particles are spherical in shape, and their particle size was 16.27 nm which means the quantity of Ag-NPs enhances as butyl acrylate concentrations increase. The formation of Ag-NPs was confirmed by UV-Vis spectroscopy, which shows an absorption peak at wavelength range 401–411 nm. FT-IR data revealed the interactions exist between butyl acrylate and Ag-NPs. The catalytic activity of Ag-NPs examined by the reduction of methylene blue and rhodamine B by Ag-NPs express extremely quick responses that change these dyes into leuco form (colorless). Conclusively, the synthesized Ag-NPs can be a promising material for the environmental remediation process.

Data availability statement

Research data will be available upon request.

CRediT authorship contribution statement

Indu Saxena: Supervision. **Syed Mohammad Ejaz:** Writing – original draft, Methodology, Data curation. **Aditya Gupta:** Writing – review & editing.

Declaration of competing interest

The authors declare the following financial interests/personal relationships which may be considered as potential competing interests: Dr. Indu Saxena reports administrative support was provided by University of Lucknow. Aditya Gupta reports writing assistance was provided by University of Lucknow. Syed Mohammad Ejaz reports a relationship with University of Lucknow that includes: funding grants and non-financial support. There is no any conflict of interest If there are other authors, they declare that they have no known competing financial interests or personal relationships that could have appeared to influence the work reported in this paper.

Acknowledgements

The authors are much grateful to the Head of the Department of Chemistry, University of Lucknow, Lucknow, India for making available laboratory for doing practical works and experiments and permitting the use of the FT-IR and UV-Vis facilities. The authors are grateful to the XRD Lab at Indore's (UGC-DAE CSR) for allowing using the XRD facilities.

Moreover, the authors are highly indebted to the Director, Birbal Shani Institute of Palaeosciences, Lucknow, UP, India for extending helping hand to provide and allow the use of FE-SEM and EDX facility. Author is also thankful to Prof. Ishwar Das (Ex. Head Gorakhpur University) for his valuable suggestions and Prof. P.C. Pandey for helping the application part.

References

- [1] Y. Sharma, P. Kapoor, Noble metal nanostructures for various applications, *Mater. Today: Proc.* 3 (2023) 628, <https://doi.org/10.1016/j.matpr.2023.03.628>.
- [2] S. Roy, A. Ghoshal, R. Panda, P. Pal, S. Ghosh, A review on bioinspired and green synthesis of silver nanoparticles with their antimicrobial activity, *J. Survey in Fisheries Sci.* 10 (1S) (2023) 6353.
- [3] B. Yaseen, C. Gangwar, R. Nayak, S. Kumar, J. Sarkar, M. Banerjee, R.M. Naik, Gabapentin loaded silver nanoparticles (GBP@AgNPs) for its promising biomedical application as a nanodrug: anticancer and Antimicrobial activities, *Inorg. Chem. Commun.* 149 (2023) 110380, <https://doi.org/10.1016/j.inoche.2022.110380>.
- [4] C. Gangwar, B. Yaseen, I. Kumar, R. Nayak, J. Sarkar, A. Baker, A. Kumar, H. Ojha, N.K. Singh, R.M. Naik, Nano palladium/palladium oxide formulation using Ricinus communis plant leaves for antioxidant and cytotoxic activities, *Inorg. Chem. Commun.* 149 (2023) 110417, <https://doi.org/10.1016/j.inoche.2023.110417>.
- [5] B. Yaseen, C. Gangwar, R. Nayak, I. Kumar, J. Sarkar, A. Baker, S. Prasad, R.M. Naik, Cannabis sativa mediated palladium nanoparticles as an effective nanodrug against multi-drug resistant bacteria and A549 lung cancer cells, *Inorg. Chem. Commun.* 157 (2023) 111254, <https://doi.org/10.1016/j.inoche.2023.111254>.
- [6] M. Österberg, K.A. Henn, M. Farooq, J.J. Valle-Delgado, Biobased Nanomaterials—The role of interfacial interactions for advanced materials, *Chem. Rev.* 123 (5) (2023) 2200, <https://doi.org/10.1021/acs.chemrev.2c00492>.
- [7] J.J. Chokkattu, S. Neeharika, M. Rameshkrishnan, Applications of nanomaterials in dentistry: a review, *J. Int. Soc. Prev. Community Dent.* 13 (1) (2023) 32, https://doi.org/10.4103/jispcd.JISPCD_175_22.
- [8] B. Yaseen, C. Gangwar, R. Nayak, J. Sarkar, R.M. Naik, Phytochemical synthesis of PdNPs utilizing *Stellaria media*/Chick weed: a Chinese medicinal herb for its antioxidant and catalytic application, *Inorg. Chem. Commun.* 155 (2023) 111058, <https://doi.org/10.1016/j.inoche.2023.111058>.
- [9] C. Gangwar, B. Yaseen, R. Nayak, A. Baker, N. Bano, N.K. Singh, R.M. Naik, Madhuca longifolia leaves-mediated palladium nanoparticles synthesis via a sustainable approach to evaluate its biomedical application, *Chem. Pap.* 77 (6) (2023) 3075, <https://doi.org/10.1007/s11696-023-02688-5>.
- [10] E. Essawy, M.S. Abdelfattah, M. El-Matbouli, M. Saleh, Synergistic effect of biosynthesized silver nanoparticles and natural phenolic compounds against drug-resistant fish pathogens and their cytotoxicity: an in vitro study, *Mar. Drugs* 19 (1) (2021), <https://doi.org/10.3390/md19010022>.
- [11] V.K. Sharma, R.A. Yngard, Y. Lin, Silver nanoparticles: green synthesis and their antimicrobial activities, *Adv. Colloid Interface Sci.* 145 (1) (2009) 83, <https://doi.org/10.1016/j.cis.2008.09.002>.
- [12] Z. Sabouri, A. Akbari, H.A. Hosseini, M. Khatami, M. Darroudi, Egg white-mediated green synthesis of NiO nanoparticles and study of their cytotoxicity and photocatalytic activity, *Polyhedron* 178 (2020) 114351, <https://doi.org/10.1016/j.poly.2020.114351>.
- [13] A. Singh, D. Jain, M. Upadhyay, N. Khandelwal, H. Verma, Green synthesis of silver nanoparticles using *Argemone Mexicana* leaf extract and evaluation of their antimicrobial activities, *Dig. J. Nanomater. Biostruct.* 5 (2010) 483.
- [14] K. Anandalakshmi, J. Venugobal, V. Ramasamy, Characterization of silver nanoparticles by green synthesis method using *Pedaliu murex* leaf extract and their antibacterial activity, *Appl. Nanosci.* 6 (3) (2016) 399, <https://doi.org/10.1007/s13204-015-0449-z>.
- [15] M. Ahmad, S. Kamyar, W. Yunus, N. Ibrahim, A.A. Hamid, M. Zargar, Synthesis and antibacterial activity of silver/montmorillonite nanocomposites, *Res. J. Biol. Sci.* 4 (2009) 1032.
- [16] E. Dabirian, A. Hajjipour, A.A. Mehri, C. Karaman, F. Karimi, P. Loke-Show, O. Karaman, Nanoparticles application on fuel production from biological resources: a review, *Fuel* 331 (2023) 125682, <https://doi.org/10.1016/j.fuel.2022.125682>.
- [17] S. Abdeen, S. Geo, S. Sukanya, P. P.K, Biosynthesis of silver nanoparticles from Actinomycetes for therapeutic applications, *Int. J. Nano Dimens. (IJND)* 5 (2014) 155.
- [18] K. Shameli, M.B. Ahmad, W.M. Yunus, A. Rustaiyan, N.A. Ibrahim, M. Zargar, Y. Abdollahi, Green synthesis of silver/montmorillonite/chitosan bionanocomposites using the UV irradiation method and evaluation of antibacterial activity, *Int. J. Nanomed.* 5 (2010) 875, <https://doi.org/10.2147/ijn.S13632>.
- [19] K. Shameli, M.B. Ahmad, W.M. Yunus, N.A. Ibrahim, Y. Gharayebi, S. Sedaghat, Synthesis of silver/montmorillonite nanocomposites using γ -irradiation, *Int. J. Nanomed.* 5 (2010) 1067, <https://doi.org/10.2147/ijn.S15033>.
- [20] B. Calderón-Jiménez, A.R. Montoro Bustos, R. Pereira Reyes, S.A. Paniagua, J. Vega-baudrit, Novel pathway for the sonochemical synthesis of silver nanoparticles with near-spherical shape and high stability in aqueous media, *Sci. Rep.* 12 (2022), <https://doi.org/10.1038/s41598-022-04921-9>.
- [21] M. Tsuji, M. Hashimoto, Y. Nishizawa, M. Kubokawa, T. Tsuji, Microwave-Assisted synthesis of metallic nanostructures in solution, *Chem. Eur. J.* 11 (2) (2005) 440, <https://doi.org/10.1002/chem.200400417>.
- [22] A.Y. Vasil'kov, K.A. Abd-Elsalam, A.Y. Olenin, K.A. Abd-Elsalam (Eds.), Green Synthesis of Silver Nanomaterials, Elsevier, 2022, pp. 241–281, <https://doi.org/10.1016/B978-0-12-824508-8.00028-9>.
- [23] R.F. Elsupikhe, K. Shameli, M.B. Ahmad, Effect of ultrasonic radiation's times to the control size of silver nanoparticles in κ -carrageenan, *Res. Chem. Intermed.* 41 (11) (2015) 8829, <https://doi.org/10.1007/s11164-015-1931-7>.
- [24] A. Gedanken, Using sonochemistry for the fabrication of nanomaterials, *Ultrason. Sonochem.* 11 (2) (2004) 47, <https://doi.org/10.1016/j.ultrsonch.2004.01.037>.
- [25] H.A. Elbadawy, A.F. Elhusseiny, S.M. Hussein, W.A. Sadik, Sustainable and energy-efficient photocatalytic degradation of textile dye assisted by ecofriendly synthesized silver nanoparticles, *Sci. Rep.* 13 (1) (2023) 2302, <https://doi.org/10.1038/s41598-023-29507-x>.
- [26] M. Vanaja, K. Paulkumar, M. Baburaja, S. Rajeshkumar, G. Gnanajobitha, C. Malarkodi, M. Sivakavinesan, G. Annadurai, Degradation of methylene blue using biologically synthesized silver nanoparticles, *Bioinorgan. Chem. Appl.* (2014) (2014) 742346, <https://doi.org/10.1155/2014/742346>.
- [27] C. He, L. Liu, Z. Fang, J. Li, J. Guo, J. Wei, Formation and characterization of silver nanoparticles in aqueous solution via ultrasonic irradiation, *Ultrason. Sonochem.* 21 (2) (2014) 542, <https://doi.org/10.1016/j.ultrsonch.2013.09.003>.

- [28] K. Satyavani, S. Gurudeeban, T. Ramanathan, T. Balasubramanian, Biomedical potential of silver nanoparticles synthesized from calli cells of *Citrullus colocynthis* (L.) Schrad, *J. Nanobiotechnol.* 9 (2011) 43. <https://doi.org/10.1186/1477-3155-9-43>.
- [29] W.M. de Azevedo, A.J.H. de Oliveira Luna, E.F.V.B.N. Silva, R.O. Silva, The effect of ultrasonic waves in conducting polymer solution, *Ultrason. Sonochem.* 13 (5) (2006) 433, <https://doi.org/10.1016/j.ulsonch.2005.10.002>.
- [30] N.A.H. Fetyan, T.M. Salem Attia, Water purification using ultrasound waves: application and challenges, *Arab. J. Basic Appl. Sci.* 27 (1) (2020) 194. <https://doi.org/10.1080/25765299.2020.1762294>.
- [31] N.V. Ayala-Núñez, H.H. Lara Villegas, L. del Carmen Ixtepan Turrent, C. Rodríguez Padilla, Silver nanoparticles toxicity and bactericidal effect against methicillin-resistant *Staphylococcus aureus*: nanoscale does matter, *NanoBiotechnology* 5 (1) (2009) 2. <https://doi.org/10.1007/s12030-009-9029-1>.
- [32] M. Li, D.-P. Yang, X. Wang, J. Lu, D. Cui, Mixed protein-templated luminescent metal clusters (Au and Pt) for H₂O₂ sensing, *Nanoscale Res. Lett.* 8 (1) (2013) 182. <https://doi.org/10.1186/1556-276X-8-182>.
- [33] H. Xu, K.S. Suslick, Sonochemical synthesis of highly fluorescent Ag nanoclusters, *ACS Nano* 4 (6) (2010) 3209. <https://doi.org/10.1021/nn100987k>.
- [34] Y. Nagata, Y. Watananabe, S.-i. Fujita, T. Dohmaru, S. Taniguchi, Formation of colloidal silver in water by ultrasonic irradiation, *J. Chem. Soc., Chem. Commun.* 21 (1992) 1620. <https://doi.org/10.1039/C39920001620>.
- [35] L. Relve, N. Nagasawa, L.Q. Luan, T. Yagi, C. Aranilla, L. Abad, T. Kume, F. Yoshii, A. dela Rosa, Degradation of carrageenan by radiation, *Polym. Degrad. Stabil.* 87 (3) (2005) 403, <https://doi.org/10.1016/j.polydegradstab.2004.09.003>.
- [36] A.M. Ruaa, S. Ghada Mohammed, A.H.M. Falah, Investigate the structural properties of silver nanoparticles produced by bio production of green spinicia oleracea leaf extract and their influence on antibacterial activity, *Iraqi J. Nanotechnol.* (3) (2022). <https://doi.org/10.47758/ijn.vi3.53>.
- [37] C. Gangwar, B. Yaseen, I. Kumar, N.K. Singh, R.M. Naik, Growth kinetic study of tannic acid mediated monodispersed silver nanoparticles synthesized by chemical reduction method and its characterization, *ACS Omega* 6 (34) (2021) 22344. <https://doi.org/10.1021/acsomega.1c03100>.
- [38] I. Kumar, C. Gangwar, B. Yaseen, P.K. Pandey, S.K. Mishra, R.M. Naik, Kinetic and mechanistic studies of the formation of silver nanoparticles by nicotinamide as a reducing agent, *ACS Omega* 7 (16) (2022) 13778. <https://doi.org/10.1021/acsomega.2c00046>.
- [39] J. Krstić, J. Spasojević, A. Radosavljević, M. Šiljegović, Z. Kačarević-Popović, Optical and structural properties of radiolytically in situ synthesized silver nanoparticles stabilized by chitosan/poly(vinyl alcohol) blends, *Radiat. Phys. Chem.* 96 (2014) 158, <https://doi.org/10.1016/j.radphyschem.2013.09.013>.
- [40] K. Shameli, M.B. Ahmad, S.D. Jazayeri, P. Shabanzadeh, P. Sangpour, H. Jahangirian, Y. Gharayebi, Investigation of antibacterial properties silver nanoparticles prepared via green method, *Chem. Cent. J.* 6 (1) (2012) 73. <https://doi.org/10.1186/1752-153x-6-73>.
- [41] H. Liu, P. Li, B. Lu, Y. Wei, Y. Sun, Transformation of ferrihydrite in the presence or absence of trace Fe(II): the effect of preparation procedures of ferrihydrite, *J. Solid State Chem.* 182 (7) (2009) 1767, <https://doi.org/10.1016/j.jssc.2009.03.030>.
- [42] C. Gangwar, B. Yaseen, R. Nayak, S. Praveen, N. Kumar Singh, J. Sarkar, M. Banerjee, R. Mohan Naik, Silver nanoparticles fabricated by tannic acid for their antimicrobial and anticancerous activity, *Inorg. Chem. Commun.* 141 (2022) 109532, <https://doi.org/10.1016/j.inoche.2022.109532>.
- [43] Y.-K. Liao, Y.-S. Lai, F. Pan, Y.-H. Su, Hybrid-biotaxonomy-like machine learning enables an anticipated surface plasmon resonance of Au/Ag nanoparticles assembled on ZnO nanorods, *J. Mater. Chem. A* 11 (21) (2023) 11187. <https://doi.org/10.1039/D3TA00324H>.
- [44] H. Huang, X. Yang, Synthesis of polysaccharide-stabilized gold and silver nanoparticles: a green method, *Carbohydr. Res.* 339 (15) (2004) 2627. <https://doi.org/10.1016/j.carres.2004.08.005>.
- [45] M. Zargar, K. Shameli, G.R. Najafi, F. Farahani, Plant mediated green biosynthesis of silver nanoparticles using *Vitex negundo* L. extract, *J. Ind. Eng. Chem.* 20 (6) (2014) 4169, <https://doi.org/10.1016/j.jiec.2014.01.016>.
- [46] K. Shameli, M.B. Ahmad, P. Shabanzadeh, E.A. Jaffar Al-Mulla, A. Zamanian, Y. Abdollahi, S.D. Jazayeri, M. Eili, F.A. Jalilian, R.Z. Haroun, Effect of Curcuma longa tuber powder extract on size of silver nanoparticles prepared by green method, *Res. Chem. Intermed.* 40 (3) (2014) 1313. <https://doi.org/10.1007/s11164-013-1040-4>.
- [47] J.R. Heath, Size-dependent surface-plasmon resonances of bare silver particles, *Phys. Rev. B* 40 (14) (1989) 9982. <https://doi.org/10.1103/PhysRevB.40.9982>.
- [48] L. Pereira, A.M. Amado, A.T. Critchley, F. van de Velde, P.J.A. Ribeiro-Claro, Identification of selected seaweed polysaccharides (phycocolloids) by vibrational spectroscopy (FTIR-ATR and FT-Raman), *Food Hydrocolloids* 23 (7) (2009) 1903, <https://doi.org/10.1016/j.foodhyd.2008.11.014>.
- [49] A. Pourjavadi, A.M. Harzandi, H. Hosseinzadeh, Modified carrageenan 3. Synthesis of a novel polysaccharide-based superabsorbent hydrogel via graft copolymerization of acrylic acid onto kappa-carrageenan in air, *Eur. Polym. J.* 40 (7) (2004) 1363, <https://doi.org/10.1016/j.eurpolymj.2004.02.016>.
- [50] K. Shameli, M. Bin Ahmad, S.D. Jazayeri, S. Sedaghat, P. Shabanzadeh, H. Jahangirian, M. Mahdavi, Y. Abdollahi, Synthesis and characterization of polyethylene glycol mediated silver nanoparticles by the green method, *Int. J. Mol. Sci.* 13 (6) (2012) 6639. <https://doi.org/10.3390/ijms13066639>.
- [51] X. Li, B. Liu, W. Ye, X. Wang, R. Sun, Effect of rectorite on the synthesis of Ag NP and its catalytic activity, *Mater. Chem. Phys.* 151 (2015) 301, <https://doi.org/10.1016/j.matchemphys.2014.11.070>.
- [52] R. Erenler, I. Hosaflioglu, Green synthesis of silver nanoparticles using *Onobrychis sativa* L.: characterization, catalytic degradation of methylene blue, antioxidant activity, and quantitative analysis of bioactive compounds, *Mater. Today Commun.* 35 (2023) 105863, <https://doi.org/10.1016/j.mtcomm.2023.105863>.
- [53] N.N. Bonnia, M.S. Kamaruddin, M.H. Nawawi, S. Ratim, H.N. Azlina, E.S. Ali, Green biosynthesis of silver nanoparticles using 'polygonum hydropiper' and study its catalytic degradation of methylene blue, *Procedia Chem.* 19 (2016) 594, <https://doi.org/10.1016/j.proche.2016.03.058>.
- [54] S.S. Emmanuel, A.A. Adesibikan, O.D. Saluu, Phylogenetically bioengineered metal nanoarchitecture for degradation of refractory dye water pollutants: a pragmatic minireview, *Appl. Organomet. Chem.* 37 (2) (2023) e6946, <https://doi.org/10.1002/aoc.6946>.